Quantum Molecular dynamics energy conservation and PHQMD

Michael Winn

Supervisor: J. Aichlein

June 20, 2019

CONTENTS

LIST OF FIGURES

CHAPTER 1

INTRODUCTION AND CONTEXT

1.1 Introduction

In most cases, heavy-ion collision simulation, relies on a mean-field approach to simulate collisions, these mean-field approaches are based on a Vlasov Botlzmann-Uehling-Uhlenbeck semi-classic model example of these are the numerical models : BUU [1, 2, 3], AMPT [4], HSD [5] GiBUU[6] and SMASH [7]. A more advance version of these that uses off-shell Kadanoff–Baym equations is PHSD [14, 15]. However the mean field models reproduce well single particle observables but they do not reproduce collective behaviour, and as that is what we would like to reproduce they are not well suited for this.

The alternative is to use a transport approach that is base on Quantum Molecular Dynamics (QMD) that propagate the particles based on a 2-body density dependent interaction such as QMD [16], IQMD [8] and UrQMD [9, 10]. Other than UrQMD (which does not have an actual potential and the cluster can not be formed after the reaction) the main disadvantage of this sort of method is that it is based on several semi-classic approximation that means that they are only applicable on low energy collision. The energy range that we can explore is that of SIS that is to say up to 1.5 GeV/A These dynamic based approaches conserve the n-body correlation and allow us to explore observables that are otherwise unavailable.

The aim of this report is to detail the addition of several new energy dependencies (notably that of momentum and asymmetry) to an already existing program. A momentum dependent potential sets this approach apart from most of the rival solution to this problem. The majority of the work achieved during this internship was focus on the improvement of the resolution and contribution to the Quantum Molecular Dynamics (QMD) [16] section of this collision algorithm. The latter is

a embedded in a overarching collision simulation called Parton Hadron String Dynamics (PHSD) [14] [15]. As this is a large code far beyond the scope of this report we shall not introduce all of what is being done, merely what is needed for this report. The fusion of this two routines is called Parton Hardron Quantim Molecular Dynamics (PHQMD) [17]. We shall then endeavour test the predictive skills of the algorithm by comparing calculated observables with experimental values notably for the cluster formation at the end of a collision [12].

1.2 Context

In the field of particle physics a number of experiments have experimentally verified the existence of Quark Gluon Plasma (QGP) in relativistic heavy ion collisions. Experimental data from RHIC and LHC experiments has given access to a number of observables of this new state of matter. However the direct study of the created plasma is not possible as they have a very short duration of existence (some $10^{-15}s$) and as such other ways of probing it are necessary. During the collision a phase transition from hadronic matter to QGP is predicted, this phase transition is of considerable interest to many field, from particle physics itself as a way of testing theories to astrophysics and the composition of neutron stars. To have a better access to this energy domain, two new particle accelerators are under construction , the Facility for Anti-Proton and Ion Research (FAIR) in Darmstadt and the Nuclotron-based Ion Collider fAcility (NICA) in Dubna.

Such observables that are needed to carry information about this cross over point are not single particles observables and as such need more sophisticate simulation to accurately predicted them. As we mentioned above, the mean field techniques used in other collision simulations obscure these n-body correlations and as such do not give us access to the observables that we wish. For the moment however our model is limited to lower energy collision and as such does not give us the ability to study the higher energies needed to produce such exotic states of matter. However as we will show in this report the success of the predictive powers of this method at lower energies will hopefully be extended to higher energies.

Other that high energy physics determination of low energy observables such as that of a gold gold collision Au+Au at 1.5 GeV/A are needed . As was shown[13] after a collision at low energy, the protons that are scattered that remain alone make up about 65% of emissions, the rest have clustered together. Collective effects can thus be studied at lower energies using this methodology.

Therefore as a first benchmark for the current iteration of the program, this report will attempt to replicate the observables (notably of cluster multiplicity for a range of impact parameters and flow) for lower energy collisions. The experimental data used as will be discussed later is from a Au+Au collision at 0.6 GeV/A.

CHAPTER 2

QMD AND ENERGY CONSERVATION

The PHQMD program is a simulation that is based on two distinct but interacting parts that are PHSD and QMD. In this type of simulation there exists two different and equally valid methods of proceeding. The first is a mean field approach which is used in PHSD the antecedent code that was used to create PHQMD. However this sort of approach does not let us study dynamic nucleon observables such as fragment distribution or flow. All of these however can in theory be predicted by a transport theory based approach where we do not solve for mean field but for and n-body theory approach with the use of 2 body interactions.

As the main aim of this simulation is to study the effects of a collision, we create two atoms (in our case gold) that are generated in the same way, referred to as projectile and target. As they are created equally anything that is valid for one is equally valid for the other.

2.1   Overview

The main routine functions on a simple loop over the time of the collision,the time step used is given by the PHSD part of the program. This means that the QMD propagation part will be explained in depth in the following report but the rest of the program will be treated. The main part of the resolution that was not studied was the collision integral that is used during our propagation. The QMD part is based mainly on a Runge-Kutta propagation that modifies the position and the momentum of each of the nuclei in our atoms (for the projectile and the target), then we re-calculate the energy of our system based on these new positions. This is done over the course of the reaction (in a typical case of 120 to 160 fm/c as an end point).

Aside It may be noted that in many case Runge-Kutta like propagation algorithms are complemented with an adaptive time step, that is to say, depending on the complexity of a given output parameter the time step is modulated such that time with a small variation in the given output are calculated faster by increasing the time step, and then decreasing it once we are once again in a zone of high fluctuations. In the original program the PHSD code it is possible to activate such a feature. However as the type of observables studied with the two approaches are completely different, the current adaptive time step is of little use to us (and the lowest value of the time step is no lower than the one used here). Furthermore the use of such methods would complicate the presentation of the energy conservation capability of the program. This is why throughout the report, a fixed time step of $0.2fm/c$ was used giving us between 600 to 800 steps depending on the chosen end point mentioned above.

In theory because all of the interactions between our nucleons are know and analytical we can gauge the conservation of the energy of our system by calculating the energy of each of the forces in question. If our system is closed then the sum of energies should be a constant during our reaction, this means that barring the numerical fluctuations and rounding we should be able to conserve the initial energy, and the loss of one part will be compensated by the gain of another. This is not however the case for all of the concerned contributions, notably that of the asymmetry, which we shall explain further one.

2.2 Initial state of the nuclei

Before we detail the various contributions to the energy of our system, we must first create it. As the aim of this program is to simulate the collision of two atoms (Au-Au) we must do the following :

- Initialise randomly in 3D space the protons and neutrons
- Verify that the binding energy of our atom would be enough to hold it together
- Launch the atoms at each other with the wanted energy, and impact parameter

2.2.1 Wood-Saxon density distribution

The nuclei are initialised with random positions but with a density distribution of protons and neutrons that relatively constant in the nucleus itself and then decreases with the radius in a Wood-Saxon manner. As we know the Wood-Saxon has the following form :

$$\rho^{WS}(r) = \frac{\rho_0}{1 + \exp\left(\frac{r - R_A}{a}\right)} \tag{2.1}$$

With the constant defined as :

- $R_A = r_0 A^{\frac{1}{3}}$ with A the number of nuclei of our nucleus (which in our case is 197 as we will always have Au nuclei)

- $r_0 = 1.125 fm$ nuclear radius

- $\rho_0 = 0.1695 fm^{-2}$ nuclear density

- $a = 0.535 fm$

The local density of our particles is calculated as follows :

$$\rho(i) = C \sum_{j \neq i}^{N} \left(\frac{4}{\pi L}\right)^{3/2} \exp\left(\frac{-4(\vec{r_i} - \vec{r_j})^2}{L}\right) \tag{2.2}$$

With $N = 197$ in our case when talking of an isolated gold atom or $N = 394$ if we are talking of the whole system i.e. two gold atoms. And L the width of our nucleon wave functions, and C a corrective factor dependent on L. And finally $\vec{r_i}$ and $\vec{r_j}$ are the positions of respectively our i^{th} and j^{th} nucleons.

At this point we can mention that for each variable we have two sums. This means that for each of our nuclei we shall calculate, the density or forces as we shall see later on based on all of the other nuclei. As such the notation that we have is that the ith value shall always be the considered nucleon and the sum over j all of the others.

On Figure 2.1, we can see the density of one of our initialised atoms (either projectile or target), each point represent the density "seen" for one of the 197 nucleons composing our atom for a given radius. Comparing this spread to our tabulated Wood-Saxon curve we can see that our nucleons are initialised correctly.
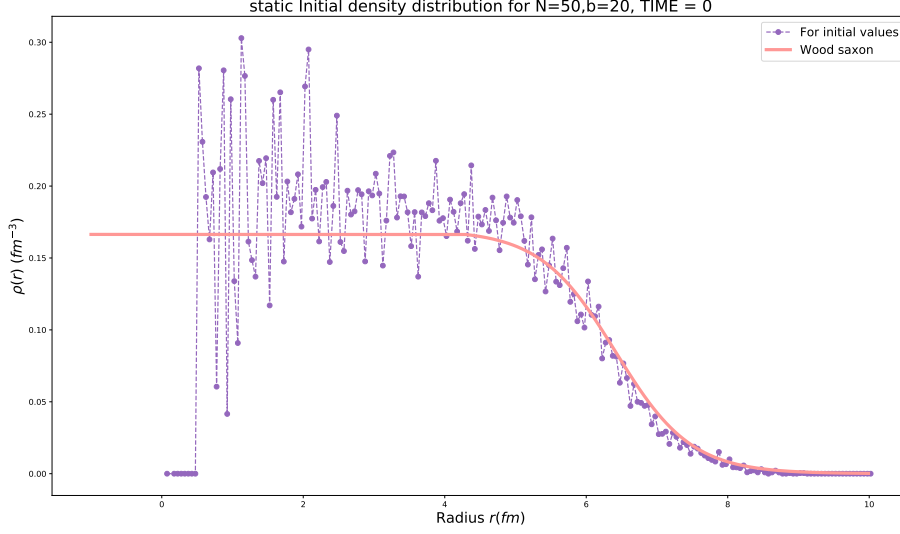
Figure 2.1: Initial density distribution $\rho(r)$ as a function of the radius of our nucleus for the static potential(purple line and markers - - -), compared with a Wood-Saxon distribution for the same radial step (Pink solid line —). Average values of N=50 iterations, at an impact parameter of b=20, at 600 Mev

2.2.2 Atomic cohesion and binding energy

As we have just seen the density of the nucleons is governed by a Wood-Saxon distribution, once the particles have been generated they are arranged within the nucleus. At this point we need to test to see if our nucleus will hold together. To ensure that we are testing only the potentials of each of our nuclei, we start by placing them at a large distance from one another (the impact parameter, b = 20 fm), such that they do not interfere with each other.

To know if this is a valid nucleus we need to calculate the binding energy of our system. Thus it is necessary to calculate the various contributions. Our initial binding energy is given by the sum of the energy contributions from the Coulomb energy, the asymmetry energy, the kinetic energy and the potential energy as follow:

$$BE^{TOTAL} = E_{kinetic}^{total} + E_{potential}^{total} + E_{coulomb}^{total} + E_{asymmetry}^{total} \qquad (2.3)$$

$$BE = \frac{BE^{TOTAL}}{A} = E_{kinetic} + E_{potential} + E_{coulomb} + E_{asymmetry} \qquad (2.4)$$

9

For ease of reading the total energy shall always be written with the superscript $TOTAL$, and would correspond to a sum over i, and the per nucleon values shall be denoted by the energy contribution type. The way in which we calculate these energies will be detailed a little further one in section 2.4. In theory the binding energy associated to a nucleus at a launching kinetic energy of 100 MeV, should be around 8 MeV per nucleon. For the two setups that we shall present here after the average values that we obtain are as follows :

Setup	Static	Momentum
Binding Energy per nucleon averaged over N= 50 Runs at an initial beam energy of 100 MeV (MeV/A)	-7.671	-7.786

Table 2.1: Average binding energy values for the two potentials that shall be detailed in section 2.4
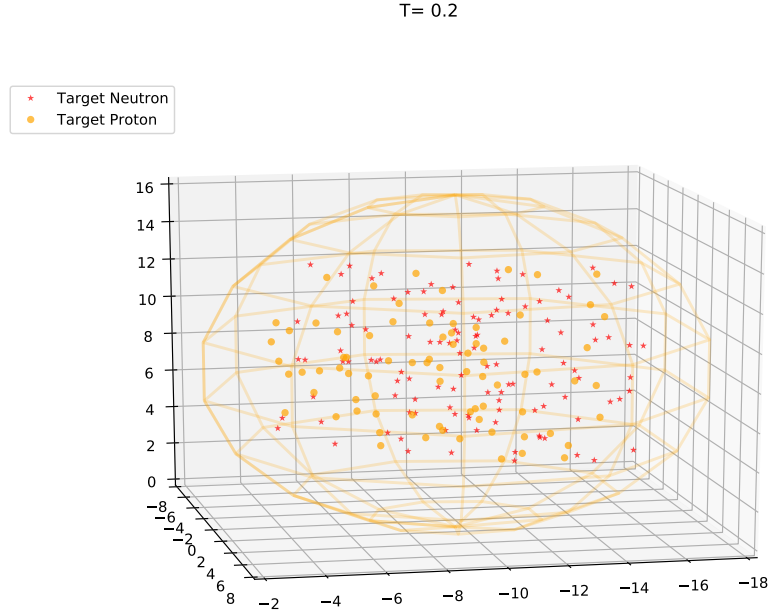

Figure 2.2: Initial distribution of the protons(orange circle •) and neutrons(red star ★) for the target nuclei, and the wire-frame sphere depicting the sphere given by the average RMS of the nucleons

Now as this is a complex situation and a lot of the code was inherited for this project we shall now focus on the work done during the internship. The aim of the latter was to improve the QMD part of this code by expanding on the way that the energy dependency is calculated. The original formulation is a static dependence, meaning that the energy of our system is independent of it's momentum. As we know this is an approximation and for higher order observables this will not do. Therefore the first step was to implement and study the momentum dependent interaction and energy an observe the impact it had on the predicted energies and densities.

2.3 Propagation

We now have an initialised system, what we need to do is update it based on the forces applied to each of the nucleons by the rest of the nucleons. To do this we shall define what we consider on of our nucleons and then calculate the propagation of particles with time.

2.3.1 Wigner Density

The chosen approach is based on an expression of our two body forces as a function of the single-particle Wigner density of each nucleon i:

$$f_i(\vec{r_i}, \vec{p_i}, t) = \sum_{j}^{N} \frac{1}{\pi^3 \hbar^3} \exp\left(-\frac{2}{L}[\vec{r}(t) - \vec{r_i}(t)]^2\right) \exp\left(-\frac{L}{2\hbar^2}[\vec{p}(t) - \vec{p_i}(t)]^2)\right) \quad (2.5)$$

Such that the expectation value of a given potential on these nucleons can be written as :

$$\langle V(\vec{r_i}) \rangle = \sum_{j}^{N} \int d^3 r_i d^3 r_j d^3 p_i d^3 p_j V(\vec{r_i}, \vec{r_j}) f_i(\vec{r_i}, \vec{p_i}, t) f_i(\vec{r_j}, \vec{p_j}, t) \quad (2.6)$$

2.3.2 Hamiltonian

To which we can apply a generalised Ritz variational principal, that allows us to write :

$$\dot{\vec{r}}(i) = \frac{\partial \langle H \rangle}{\partial \vec{p}(i)} \quad (2.7)$$

$$\dot{\vec{p}}(i) = \frac{\partial \langle H \rangle}{\partial \vec{r}(i)} \quad (2.8)$$

With $\langle H \rangle$ the Hamiltonian of our system that we can decompose as follows:

$$\langle H \rangle = \langle T \rangle + \langle V \rangle \quad (2.9)$$

With $\langle T \rangle$ the kinetic contribution to our system and $\langle V \rangle$ the potential. The potential energies added in this setup are as follows:

$$V_{i,j}(\vec{r_i}, \vec{r_j}) = V_{skyrme} + V_{Coulomb} + V_{asymmetry} \quad (2.10)$$

To each of these potential is linked a force, that can be written :

$$\vec{F}_V = -\vec{\nabla} V \quad (2.11)$$

2.3.3   Runge-Kutta RK(4)

Now that we can express the potentials applied to each of the nucleons and we can calculate the forces that they will have on our particles, we must proceed to a method to propagate the new values given for the position and the momentum by Eq. (2.8).

In our case the Runge-Kutta is used to recalculate the position and the momentum of all of our nucleons (both in the target and the projectile). To do so we must know the energy contribution of each of the different potentials applied to our system, a detailed breakdown of each is given in Section 2.4. As this is necessary to understand the setup of our system we shall present it beforehand.

As we have mentioned previously our time step is fixed with a value of $\Delta t = 0.2fm/c$. As indicated by the rank the RK(4) uses four evaluation per time step, this means that at each time step we calculate the following :

$$
\begin{cases}
f_1 = F(t, \vec{r}, \vec{p}) \\
f_2 = F(t + \Delta t/2, \vec{r} + f_1(\vec{r})/2, \vec{p} + f_1(\vec{p})/2) \\
f_3 = F(t + \Delta t/2, \vec{r} + f_2(\vec{r})/2, \vec{p} + f_2(\vec{p})/2) \\
f_4 = F(t + \Delta t, \vec{r} + f_3(\vec{r}), \vec{p} + f_3(\vec{p}))
\end{cases}
\tag{2.12}
$$

Where F corresponds to the update function that allows us to recalculate all the forces applied each of our nucleons.

$$
F(i) = \sum_j^N F_{skyrme}(i,j) + F_{Coulomb}(i,j) + F_{asymmetry}(i,j)
\tag{2.13}
$$

With this four values we can calculate the propagation that is to be applied to each of the coordinates and momentum as follows :

$$
\vec{r} \rightarrow
\begin{cases}
x(t + \Delta t) = x(t) + \Delta t \left(\frac{f_1(x)}{6} + \frac{f_2(x)}{6} + \frac{f_3(x)}{3} + \frac{f_4(x)}{6} \right) \\
y(t + \Delta t) = y(t) + \Delta t \left(\frac{f_1(y)}{6} + \frac{f_2(y)}{6} + \frac{f_3(y)}{3} + \frac{f_4(y)}{6} \right) \\
z(t + \Delta t) = z(t) + \Delta t \left(\frac{f_1(z)}{6} + \frac{f_2(z)}{6} + \frac{f_3(z)}{3} + \frac{f_4(z)}{6} \right)
\end{cases}
\tag{2.14}
$$

$$
\vec{p} \rightarrow
\begin{cases}
p_x(t + \Delta t) = p_x(t) + \Delta t \left(\frac{f_1(p_x)}{6} + \frac{f_2(p_x)}{6} + \frac{f_3(p_x)}{3} + \frac{f_4(p_x)}{6} \right) \\
p_y(t + \Delta t) = p_y(t) + \Delta t \left(\frac{f_1(p_y)}{6} + \frac{f_2(p_y)}{6} + \frac{f_3(p_y)}{3} + \frac{f_4(p_y)}{6} \right) \\
p_z(t + \Delta t) = p_z(t) + \Delta t \left(\frac{f_1(p_z)}{6} + \frac{f_2(p_z)}{6} + \frac{f_3(p_z)}{3} + \frac{f_4(p_z)}{6} \right)
\end{cases}
\tag{2.15}
$$

For a quick summary of what is being done we can look at the following flowchart:
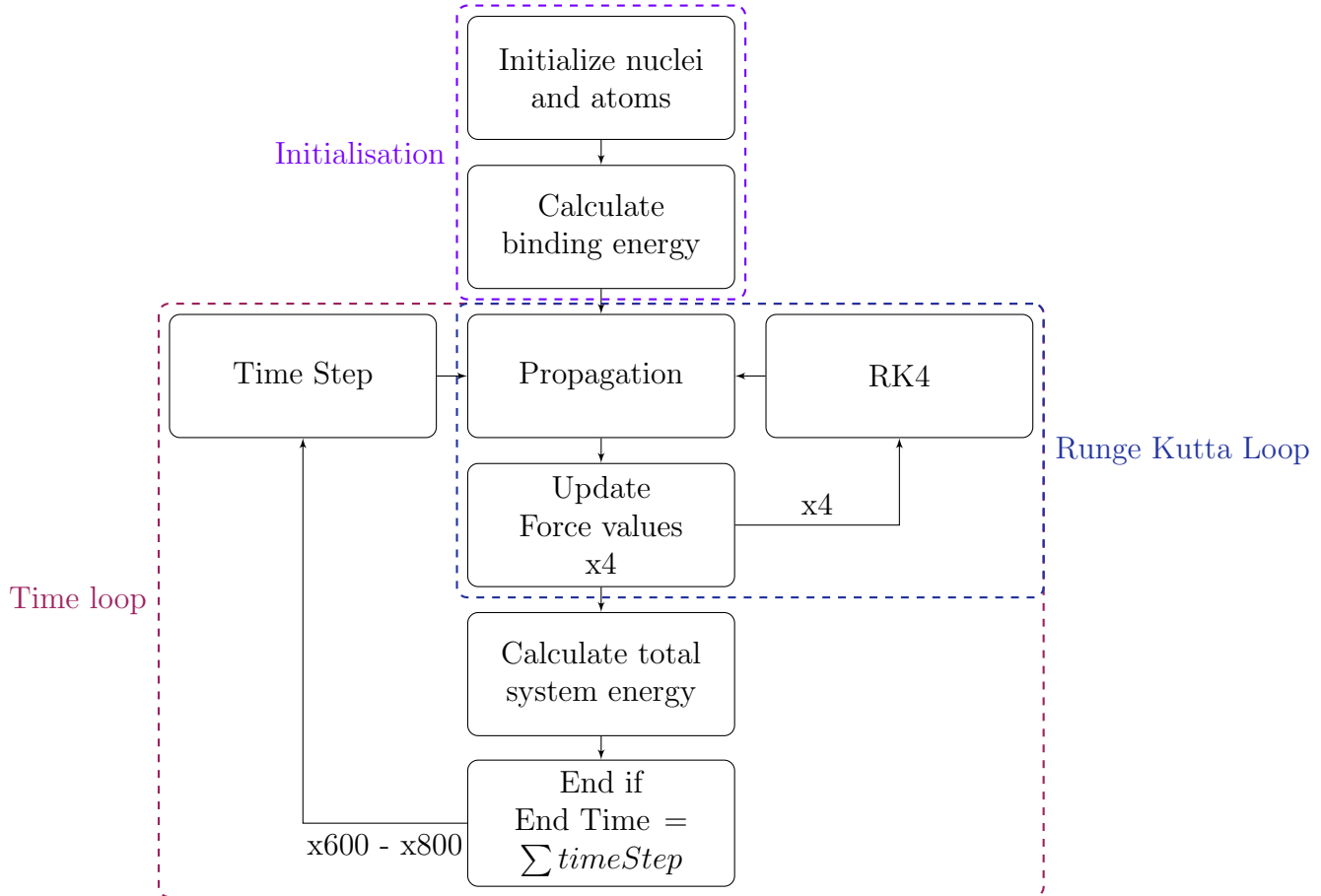

Figure 2.3: Simple diagram of the algorithmic process

For each loop of the Runge-Kutta we call our force update function, and for each time loop we call the latter 4 times and the energy function once. This means that the update function is called up to 3200 times, in the simplest case, however as we shall see later on that other contributions Section 2.4.1, mean that the update function will be called several hundreds of thousands of times and the internal loops on the nuclei themselves, several million times. Now that we have presented the main algorithmic processes behind this simulation we shall detail how each of the energies and forces are computed at each time step.

2.4 Energy contributions

As the program is based on a molecular dynamics style calculation, we calculate for each particle the effect of every other particles in our nucleus. For each of the following effects we shall proceed in the same manner that is to say that we shall at first define the potential and potential energy of the given energy contribution then the force that derives from it As we noted before for each of the potential we have the force :

$$\vec{F}_V = -\vec{\nabla} V \tag{2.16}$$

All of the forces and energies that are used are between two particles, for they are all based on two-body forces, this means that the energy will always be preceded by a factor $\frac{1}{2}$, as well as all the other constants.

The energy associated shall be denoted by $e_V(i)$, as the contribution of the i^{ith} nucleon, and E_V as the total per nucleon average of that given energy such that:

$$E_V = \frac{1}{N} \sum_i^N e_V(i) \tag{2.17}$$

This means that if we have an analytical expressions for the potential generated by each of the particle we can find the analytical expression of the applied force.

2.4.1 Kinetic contribution

As we mentioned previously the collision integral that determines the elastic collision between two of our nuclei is inherited from the PHSD part of the program and as such was not implemented by the author of this report. The verification of the conservation of the kinetic energy is a formality in this case as the existing program is know to function.

If we strip our system of all other properties we are left with the collision of two sphere and their components (i.e. protons and neutrons). As we view our system as closed, this gives rise to the fact that this reaction can be analytically simulated and as such we should conserve perfectly the total energy of our system. The kinetic energy of each nucleon of our system can be written as :

$$e_c(i) = \sqrt{p_x(i)^2 + p_y(i)^2 + p_z(i)^2 + m_0(i)^2} - m_0^2(i) \tag{2.18}$$

With $p_{x,y,z}$ the respective impulse contribution on each axis, and m_0 the rest mass of either the proton or the neutron.

The total average energy of our system at a time t is the sum of all the energetic contributions, in this case that will only be from the kinetic energy of all of our nuclei at that same time t.

$$E_{kinetic}(t) = \frac{1}{N} \sum_i^N e_c(i) \tag{2.19}$$

Ensemble Calculations To diminish the statistical fluctuations, each event is run over a number of runs in the same initial conditions and the average values of that number of runs are given , such that the kinetic energy average becomes :

$$E_{kinetic}(t) = \frac{1}{N_{NUM}} \sum_k^{N_{NUM}} \frac{1}{N} \sum_i^N e_c^k(i) \tag{2.20}$$

This means that for each time step we recalculate the values N_{NUM} times. For all the graphs in the following section we have a number of runs $N_{NUM} = 20$, and for the production runs that we shall use to study the observables in Chapter 3 we increase this number to 40. The force contribution for the kinetic component is the simplest as we have no position dependency as such the equation Eq. (2.8) becomes:

$$\dot{\vec{r}}(i) = 0 \tag{2.21}$$

$$\dot{\vec{p}}(i) = \frac{\partial \langle T \rangle}{\partial \vec{r}(i)} \tag{2.22}$$

The resulting force is therefore only on the momentum components such that :

$$F_{\vec{r}}(i, \vec{p}) = \frac{\vec{p}(i)}{E} \tag{2.23}$$

In the following graph we present the total energy of our system on the left, and the part of it, that is due to the kinetic energy on the right. This shall be the case with the rest of the contributions that we shall show the split contribution of each of our energy components.
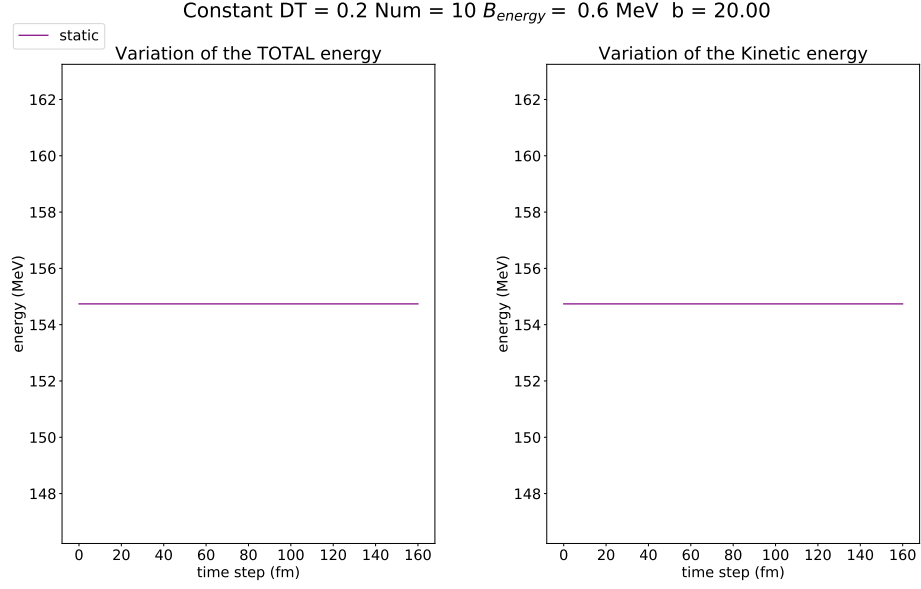
Figure 2.4: Conservation of the system energy with the total system energy (right) and kinetic energy (left) as a function of the time of the collision for a large parameter of impact b = 20 fm, and for a ensemble run of N = 20, at a launching energy of 600 MeV

As we can see there are no fluctuations in the energy of our system and we resolve the collision integral without loosing any energy. This also means several other things:

- Firstly that the Runge-Kutta that segments our simulation into time steps is of the appropriate order (RK4) for the task and that is it functioning correctly

- That the chosen time step for the algorithm is small enough to conserve the energy of our system without being so small as to add numerical errors

- That the collision integral is functioning perfectly

All of this being the case we can move onto the next energetic contribution to our system.

2.4.2   Potential contribution

The second energy contribution that we shall detail is that of the potential energy. The potential is base on a Skyrme type potential for the static part and an fitted optical potential for the momentum dependence.

The potential contribution to the energy of our system can be split into two parts, the static contribution and the momentum dependent contribution,the poten-

tial can be written as a Skyrme like interaction as:

$$V(\rho) = \alpha\rho + \beta\rho^\gamma + V_{momentum}(\rho) \tag{2.24}$$

And thus the energy associated to this is :

$$E_{pot} = \boxed{\frac{\alpha}{2}\rho + \frac{\beta}{2(\gamma+1)}\rho^\gamma} + \boxed{\frac{1}{\rho}\int V_{momentum}d\rho}$$
$$\underbrace{\phantom{\frac{\alpha}{2}\rho + \frac{\beta}{2(\gamma+1)}\rho^\gamma}}_{\text{static part}} \quad \underbrace{\phantom{\frac{1}{\rho}\int V_{momentum}d\rho}}_{\text{momentum part}}$$
$$= E_{static} + E_{momentum} \tag{2.25}$$

Static Hard and Soft

We shall return to the description of the momentum potential in a moment. This separation allows us to study the effect of the momentum dependent part on the observables of out system. As such it is necessary to have two sets of parameters(α β γ) to be able to separate the two. We dispose of a sufficient number of properties that the potential much satisfy to be able to determine these three values. It must obey the following :

- $E/A(\rho = 1) = -16 MeV$

- $\frac{\partial E/A}{\partial\rho}|_{\rho=1} = 0\, MeV$

- $K = 9\rho^2\frac{\partial P}{\partial\rho} = 200$ For the soft equation of state or

- $K = 9\rho^2\frac{\partial P}{\partial\rho} = 380$ For the hard equation of state

We can thus solve the equations given above and obtain two parametrisations of the potential contribution in the static form, for the hard EoS and the soft EoS. We obtain the following set of parameters

EoS	Soft	Hard
$\alpha(MeV/c^2)$	-383.5	-125.3
$\beta(MeV/c^2)$	329.5	71.0
γ	1.15	2.0

As we wrote previously the local density in Eq. (2.2) for each of our nucleons is written :

$$\rho(i,t) = C\sum_{j\neq i}^{N}\left(\frac{4}{\pi L}\right)^{3/2}\exp\left(\frac{-4(\vec{r_i}-\vec{r_j})^2}{L}\right) \tag{2.26}$$

This means that for each nucleon we can write :

$$e_p(i,t) = \alpha\rho(i,t) + \frac{\beta}{\gamma+1}\rho(i,t)^\gamma \tag{2.27}$$

Therefore the total average potential energy of our system is given by :

$$E_{potential}(t) = \frac{1}{N} \sum_{i}^{N} e_p(i,t) \tag{2.28}$$

The derived force for this energy would be :

$$F_{\vec{p}}(i) = \mathcal{C} \sum_{j}^{N} (r(\vec{i}) - r(\vec{j})) \exp\left(\frac{-4(\vec{r_j} - \vec{r_i})^2}{L}\right) \left[\alpha_f + \frac{\beta_f \gamma}{\gamma(\gamma+1)}(\rho(i)^{\gamma-1} + \rho(j)^{\gamma-1})\right] \tag{2.29}$$

With $\mathcal{C}$ taking care of the constants that appear out of the derivation of the energy, and the $\alpha_f \propto \alpha$ and $\beta_f \propto \beta$, with some constants to simplify notation Applying this to our system as well as the kinetic energy we get the following :
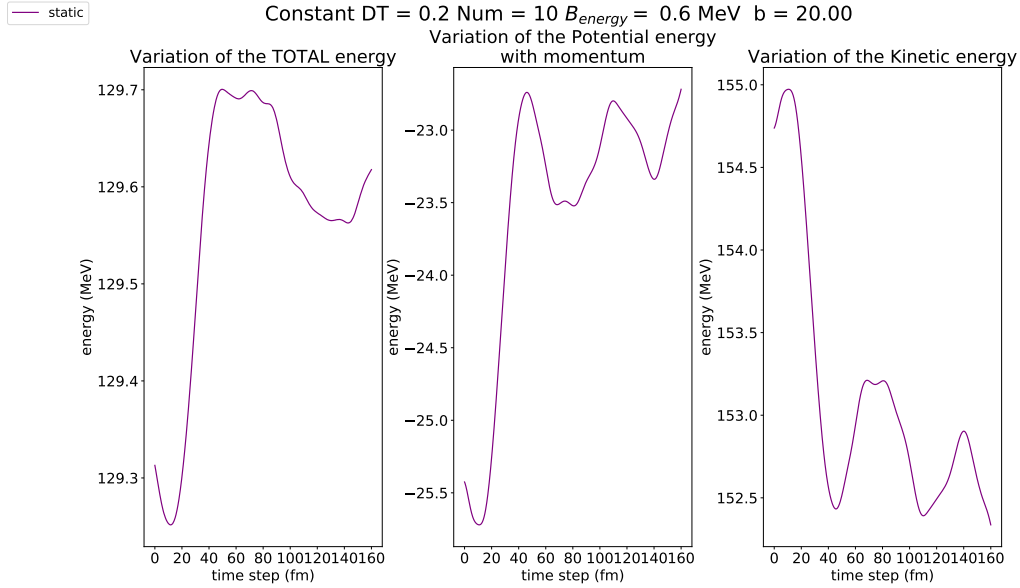

Figure 2.5: Total average energy (right) Total average potential energy(center) and total average kinetic energy(left) as a function of the time of the collision for a large parameter of impact b = 20, and for a ensemble run of N = 20, at a launching energy of 600 MeV

As we can see the potential is converted from the kinetic energy as it loose energy, the potential well becomes shallower. And our total energy remains approximately constant varying by less than 0.5 %.

Momentum

The momentum part of the potential contribution will be given by and optical potential that was fitted on experimental values for the measured kinetic energy [11]. The contribution of the potential is then added to the previous expression of the potential energy. Which gives us:

$$V(\rho) = \alpha\rho + \beta\rho^\gamma + V_{momentum}(\rho) \qquad (2.30)$$
$$= V_{static} + V_{momentum} \qquad (2.31)$$

The optical potential is a fitted expression with the following expression :

$$V_{opt} = \exp\left(-c\sqrt{(p(\vec{i}) - p(\vec{j}))^2}\right)\left(a(p(\vec{i}) - p(\vec{j}))^2 + b(p(\vec{i}) - p(\vec{j}))^4\right) \qquad (2.32)$$

With the parameters having the values :

- $a = 236.326(MeV/c^2)^{-1}$

- $b = -20.7304(MeV/c^2)^{-2}$

- $c = 0.901519MeV^{-1}$

And $p(\vec{i})p(\vec{j})$ the respective i^{th} nucleon j^{th} nucleon's momentum. Thus this gives rise to another set of parameter that correspond to the which we shall condier the full potential expression:

EoS	Soft
$\alpha(MeV/c^2)$	-478.87
$\beta(MeV/c^2)$	413.76
γ	1.10

The force deriving from this expression of the potential is also separated into two parts, with the static part being having the same expression as in Eq. (2.29), and as this potential introduces a dependence on the momentum we have the addition of :

$$F_{\vec{r}}(i) = \mathcal{C}\sum_j^N(\vec{p}(i) - \vec{p}(j))\exp\left(\frac{-4(\vec{r_j} - \vec{r_i})^2}{L}\right)\exp\left(-c\Delta p(i,j)\right) \qquad (2.33)$$
$$\left(2a - c(a + b\Delta p)\sqrt{\Delta p} + 4b(\Delta p)\right)$$

With $\Delta p = (\vec{p}(i) - \vec{p}(j))^2$, and $\mathcal{C}$ the constants due to the derivation

In this report we are not going to study the hard momentum dependent potential, to illustrate why we shall look at the Equations of State (EoS) given for each of these potentials. The simple analogy is that the hard EoS is more repulsive and

pushes our nuclei apparent than the soft. However the addition of the momentum dependence means that creates a more repulsive potential. We can plot the equation of state for these three equations and justify this choice.
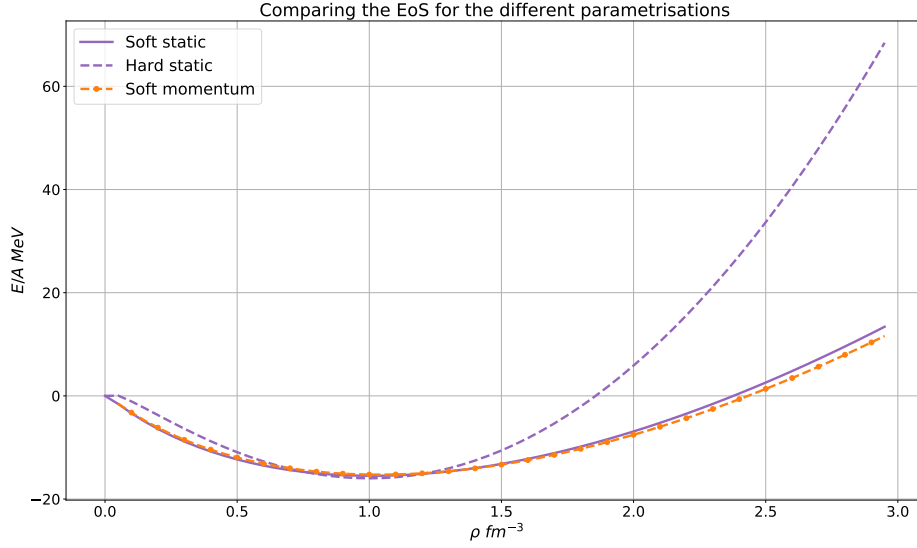

Figure 2.6: Comparing the energy per nucleon of three equations of state(EoS), soft static EoS (purple line ——), hard static EoS (purple dotted line - - -) and soft momentum EoS (Orange dotted line and markers - - -)

As we can see the EoS for the soft static, and the soft momentum are very similar. At normal nuclear matter density we have similar values for all three.

Now that we have ascertained the difference between our potentials we can check the conservation for all three parameter sets.
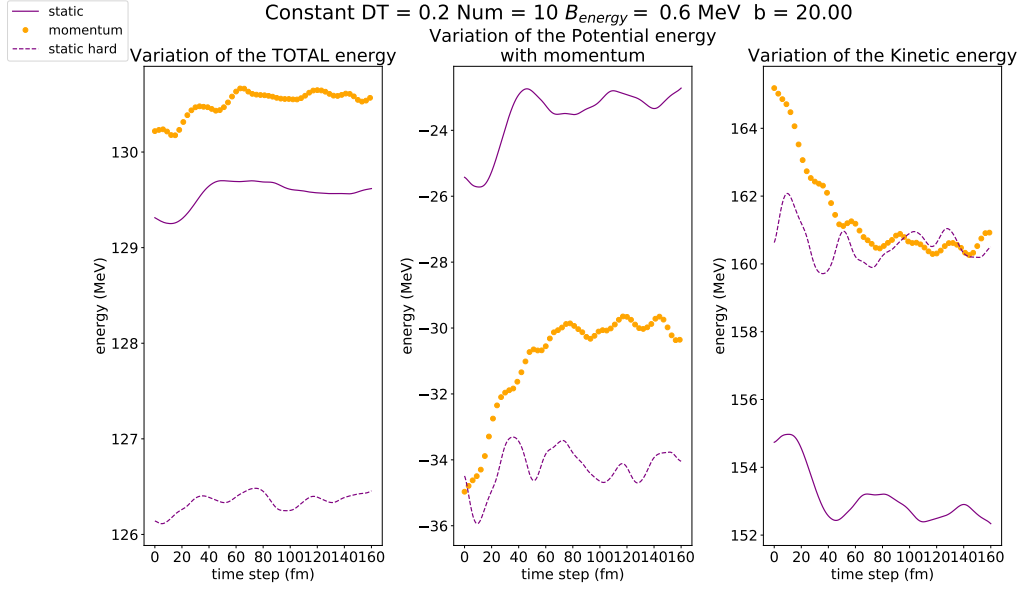
Figure 2.7: Total average energy (left), Total average potential energy (centre), Total average kinetic energy (right) in function of collision time. This is done for static soft (purple line —), static hard (- - -) and momentum (orange markers •).

As can be seen which every potential used, the energy conservation via the routine is approximately the same, save the fact that the starting energies differ because of the strength of our potentials.

However a previous version of this momentum contribution had been added in the past. This contribution was a different fit on the same data set but using a different functional form :

$$U_{opt} = -54 + 1.58\ln\left[(p(i) - p(j))^2 a + 1\right]^2 \tag{2.34}$$

Therefore we can compare the new parametrisation of the fitted data with the previous version in order to verify that we have similar behaviour, as the two are based on the same idea.
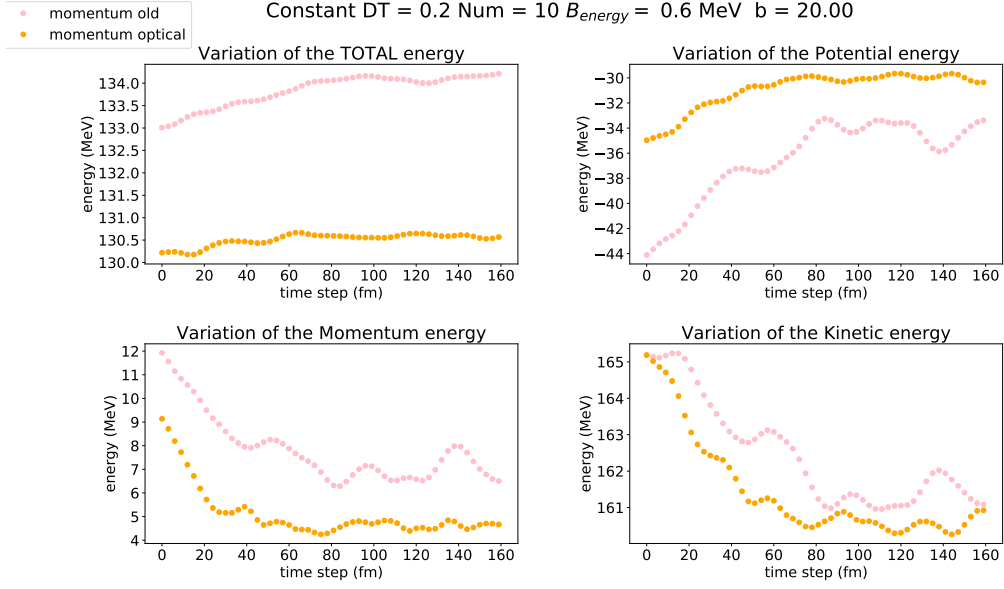
Figure 2.8: Total average energy (top left), Total average potential energy (top right),Total average momentum energy (bottom left) Total average kinetic energy (bottom right) in function of collision time. This is done for the previous version of the momentum dependence(pink •) , and the current optical potential version (orange •) .

As can be seen in the above figure, both of the momentum based potentials give similar results. The conservation of the energy is not perfectly conserved at the early time step, this is because the lose of energy from momentum to kinetic happens quite quickly and the Runge-Kutta losses some on the way. At larger times when the variation has slowed the energy fluctuates considerably less.

The overall contribution of the momentum potential is somewhat lower in this newer parametrisation by about 2 Mev/A. This being said, as it is supposed to be a more accurate representation of the experimental data, it is the version with which shall continue.

2.4.3 Coulomb Contribution

The next energy contribution we shall look at is that of the Coulomb energy. To do so we calculate the exact analytical Coulomb potential between two charged

particles, such that the potential can be written :

$$I = \frac{a^{3\,3}}{\pi^3} \int d^3r_i d^3r_j \exp(-a(r(\vec{i}) - r(\vec{i})_0))^2) \exp(-a(r(\vec{j}) - r(\vec{j})_0))^2) \frac{1}{\left| r(\vec{i}) - r(\vec{j}) \right|} \tag{2.35}$$

This gives us :

$$e_{coulomb}(i) = \frac{1}{2} \frac{\mathrm{Erf}\left(\sqrt{a/2}\sqrt{(r(\vec{i}) - r(\vec{j}))^2} \right)}{\sqrt{r(\vec{i}) - r(\vec{j})}} \tag{2.36}$$

Thus as previously we can express the total average contribution to our system:

$$E_{Coulomb} = \frac{1}{N} \sum_i^N e_{Coulomb}(i) \tag{2.37}$$

The associated force is :

$$F_{\vec{p}}(i) = \mathcal{C} \sum_j^N -(r(\vec{i}) - r(\vec{j})) \left[\sqrt{\frac{2a}{\pi}} \frac{\exp(-\frac{a}{2}\Delta^2)}{\Delta^2} - \frac{\mathrm{Erf}(\sqrt{a/2}\Delta)}{\Delta^3} \right] \tag{2.38}$$

With $\Delta = \sqrt{(r(\vec{i}) - r(\vec{j}))^2}$, and some constants $\mathcal{C}$.
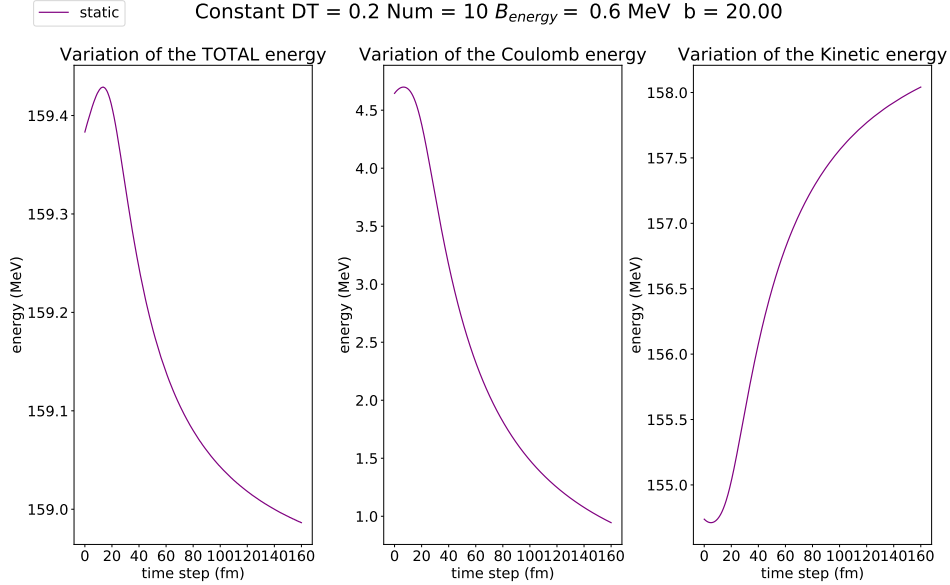

Figure 2.9: Total energy (left), Total Coulomb energy (center), Total Kinetic energy (right) for the static potential.

The Coulomb energy contribution is one of the most numerically intensive(along with the asymmetric contribution that we will get to next) of the energy contributions as it requires to be calculated at each ith position j times, as well as using a none analytical function that is the error function.

Asymmetry Contribution

The final contribution is that of the asymmetry energy. By analogy with the Bethe-Weizscker forumla we know we have a contribution from the asymmetry contribution of the protons and neutrons to our system should have the following form :

$$E_{asym}^{BW} = \frac{\sum_i^N e_{asym}(i)}{A} = \sum_i^N C \left(\frac{\rho_p(i) - \rho_n(i)}{\rho_p(i) + \rho_n(i)} \right)^2 (\rho_p(i) + \rho_n(i))^\delta \qquad (2.39)$$

$$= \sum_i^N C(\rho_p(i) - \rho_n(i))^2(\rho_p(i) + \rho_n(i))^{\delta-2} \qquad (2.40)$$

Deriving this with respect to ρ to obtain the potential we have :

$$U_{asym}(\rho) = \frac{\partial \tilde{U_{asym}}}{\partial \rho} = \sum_i^N [2(\rho_p(i) - \rho_n(i))(\rho_p(i) + \rho_n(i))^{\delta-2} + \qquad (2.41)$$

$$(\delta - 2)(\rho_p(i) - \rho_n(i))^2(\rho_p(i) + \rho_n(i))^{\delta-3}]$$

However this rapidly becomes rather complicated, therefore a different approach was used. Instead of considering the densities, we should consider the ratio of the protons to neutrons, such that :

$$\left(\frac{\rho_n(i) - \rho_n(i)}{\rho_p(i) + \rho_n(i)} \right)^2 \rightarrow \left(\frac{Z - N}{Z + N} \right)^2 \qquad (2.42)$$

And so the potential energy becomes

$$\tilde{U_{asym}} \propto \sum_i \frac{\sum_j TZ(i)TZ(j)\exp(-a(r_{io} - r_{jo})^2)}{\sum_j \exp(-a(r_{io} - r_{jo})^2)} \rho(i)^\delta \qquad (2.43)$$

With TZ the sign of the consider particle , with :

- $TZ(i) = 1$ if i is a proton
- $TZ(i) = -1$ if i is a neutron

As one can see this contribution is even more numerically taxing than the last, needing the two sums over j (from j to N) as well as the third sum over j done for

the density. The associated force is :

$$F_{\vec{p}}(i) = \mathcal{C} \sum_{j}^{N} \exp\left(\frac{-4(\vec{r_j} - \vec{r_i})^2}{L}\right) \rho(i)^{\delta-1} \frac{\sum_{j} \mathrm{TZ(i)TZ(j)} \exp\left(\frac{-4(\vec{r_j}-\vec{r_i})^2}{L}\right)}{\rho(i)} \quad (2.44)$$
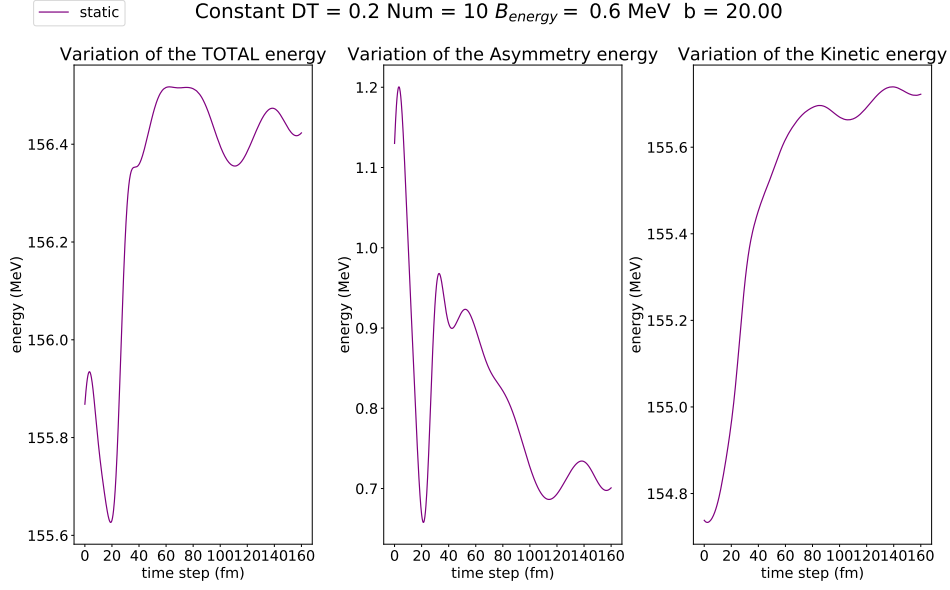

Figure 2.10: Total energy (left), Total Asymmetry energy (center), Total Kinetic energy (right) for the static potential.

Of all of the contributions this is the least stable, as we can see we have a far larger energy fluctuation in the order of $2\,Mev/A$, this is most likely due to a combination of factors, the none analytical form of the energy and thus the force will introduce small errors that will be amplified by the small time step of our Runge-Kutta, and the speed of the variation as which is faster than most of the other contributions, and exists throughout the collision. As the asymmetric energy is proportional to the product of the signs of the considered nuclei (+1 for protons and -1 for neutrons) we see swings in individual contributions as from the ith value to the next as the behaviour changes.

2.5 Total energy contributions

As a final step we can make sure that when all of the contributions are added, that the overall energy is conserved throughout our reaction. Once again this is done at height impact parameter.
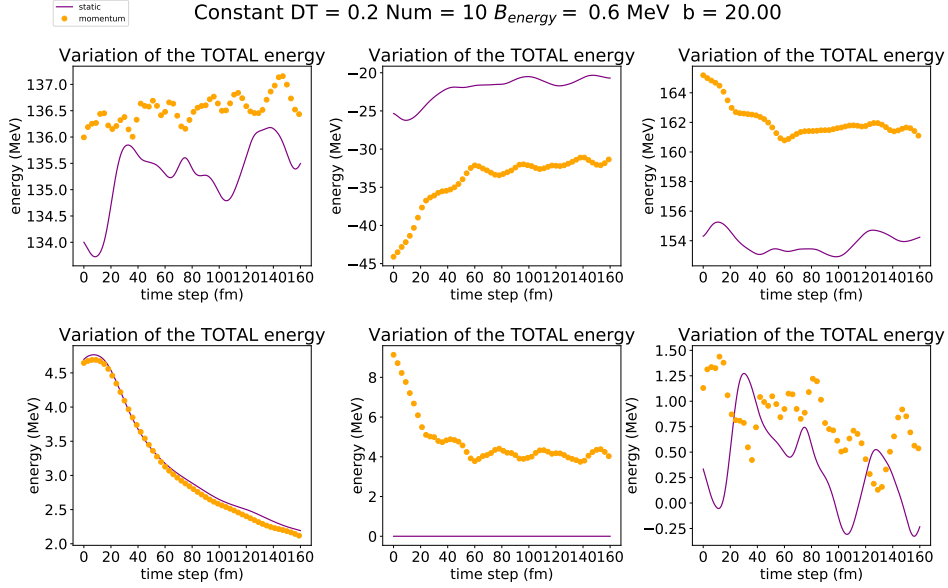

Figure 2.11: Total energy conservation for a full run at 600 Mev, with a large impact parameter b =20, for N=20 runs. On the top row from left to right we have the Total energy of our system, the potential energy, the Kinetic energy. On the bottom row, we have the Coulomb energy, the Momentum energy and the asymmetry energy. This is presented for the static potential(purple line —) and the momentum potential (orange marker •)

2.5.1 Destabilising effect of the asymmetry contribution

It is worth noting that the main contribution to the loss of energy conservation in the current setup is the asymmetry energy. If we proceed to the same plot as we have just above, with the omission of the asymmetric contribution, we can see that the energy is considerably more stable:
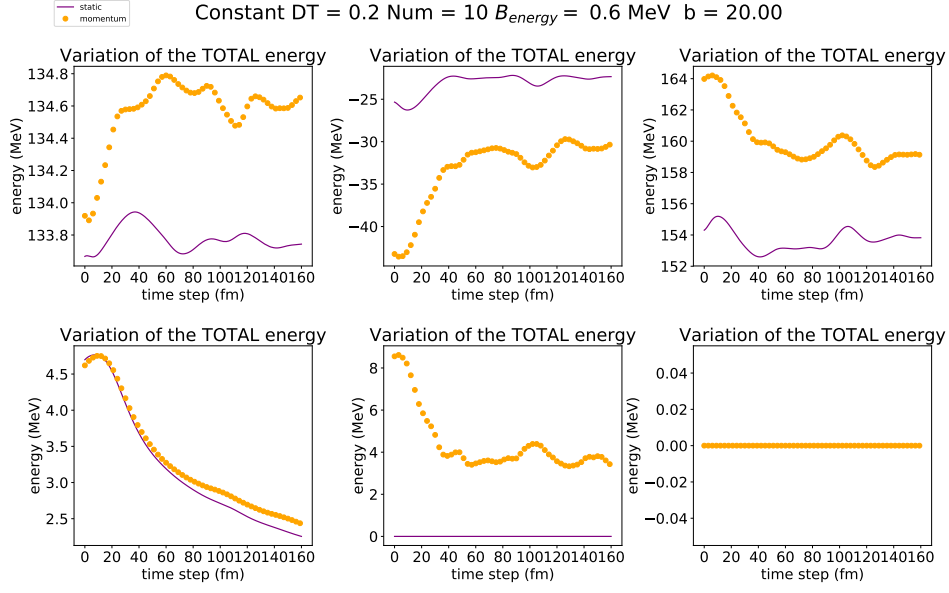
Figure 2.12: Same as Figure 2.11 with the asymmetric contribution turn off

As we see we have a smaller degree of fluctuations. This is somewhat expected as the asymmetric contribution is the only truly none analytical addition that we have and so can not be exactly conserved. This is only amplified by our Runge-Kutta time step that is relatively small and thus enhances this effect. This means that in this configuration the energy loss over our collision time is of the order of 0.7 %.

This means that even in the full setup the total variation in our energy is on the order of 2 %. Which for the current application is acceptable.

2.5.2 Low impact parameter collision

The final case we shall check is the conservation during the much more complicated head on collision, as the two nuclei collide their protons and neutrons are thrown out of the nucleus and scatter much more dramatically than in a glancing blow.
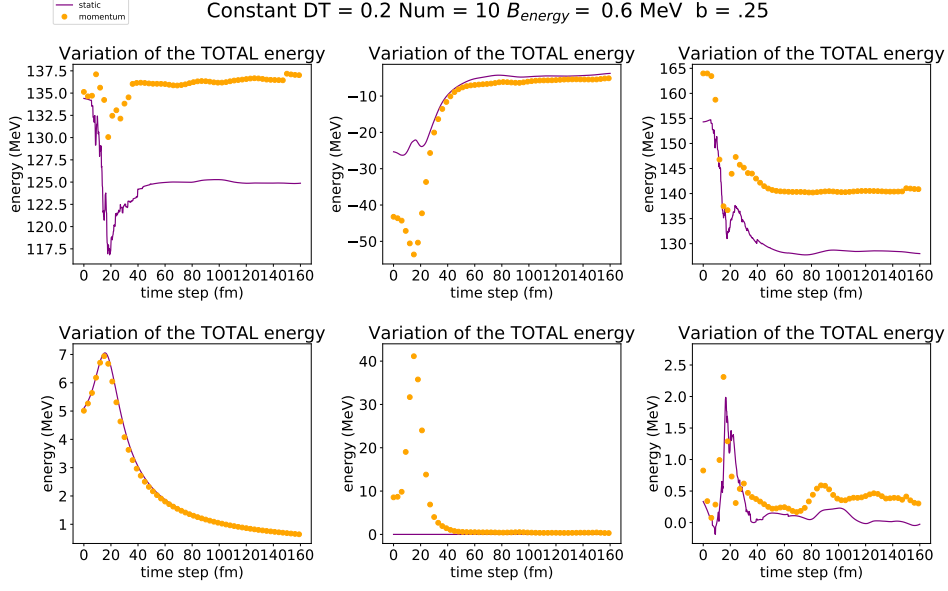
Figure 2.13: Same as Figure 2.11 an impact parameter of b=0.25, this is a head on colision

Fig. 2.13 show on of the main weaknesses of the current setup. During a head on collision the energy loss spikes and we present some strange behaviour in both static and momentum, with very sharp changes in the kinetic energy leading to losses by the Runge-Kutta. This is mainly due to two factors :

- The time step may not be entirely adequate during the collision itself, and thus we loss some energy from this

- The main problem is the way we calculate the density.

As it stands the density is calculated in a scalar fashion. However as the collision illustrates that to have a correct relativistic calculation we must calculate the density quadri-vector and ascertain the vector and scalar parts of our potential interaction. Such an overhaul of the methods used was not possible in the duration of this internship, but such modifications will be made in the future. We must content ourselves with an energy loss of around 8 % during the collision. After which the system returns to the normal fluctuations.

CHAPTER 3

OBSERVABLES

3.1 Overview

Now that we have a more complex framework for the calculation of our energy throughout the collision of our nuclei, we can look at the difference in the predictive power of our two models. Here we shall compare some of the notable observables of the collision.

3.2 Fragment Multiplicity

One of the observables that we can study is the charged fragment multiplicity. After the collision the remaining nucleons cluster together or fly off. This quantity has been experimentally observed for an energy range of 600 - 1000 Mev/A [12]. This is within our domain of validity of our semi-classic approximations that we use for our dynamic propagation. This means that we have experimental values with with we can directly compare our predictions.

3.2.1 Static distribution

Soft EoS

As we have discussed previously, the static potential has two different parameter sets, this means that we will obtain two sets of results for our fragment distribution. The first that we shall show if the soft equations of state
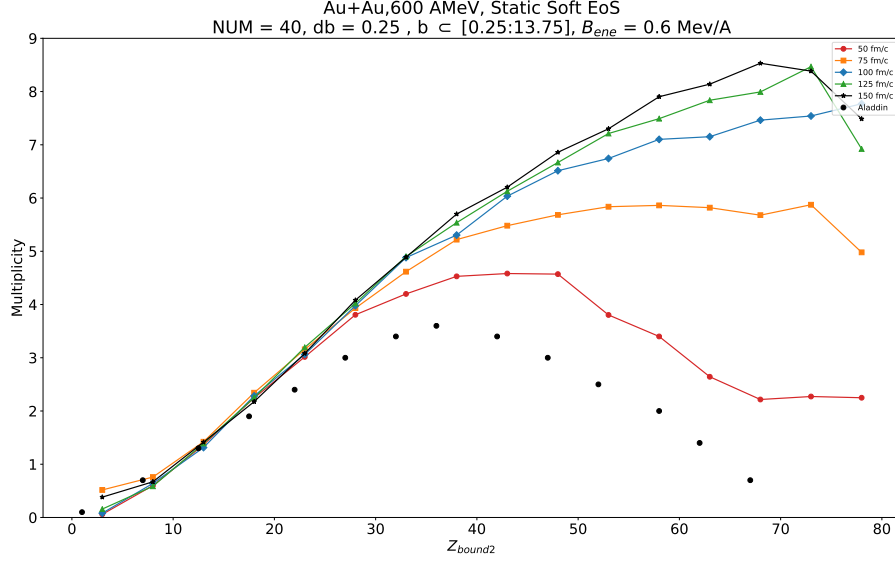
Figure 3.1: Fragment distribution in number as a function of the charge contained, the dots are the experimental values that were obtained from [12], and the lines are the distributions that we obtain at several different times during the collision

As we can see at the early stages of the collision we reproduce well the expected distribution but our nuclei loose cohesion and fragment into much greater number that what we would expect compared to the experimental data

Hard EoS

As we saw on the EoS state comparison 2.4.2, the hard and momentum dependent interaction are very similar around the nuclear saturation density. And as such the hard EoS is a good substitute for the momentum dependent version as we can see by the fact that is reproduces the experimental values for the whole collision, and does not break up at the end of the collision.
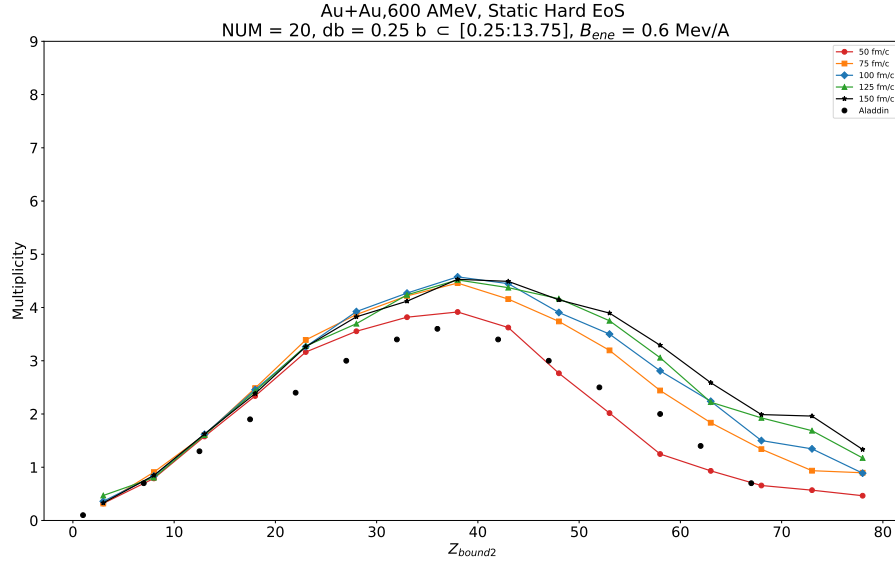
Figure 3.2: Fragment distribution in number as a function of the charge contained, the dots are the experimental values that were obtained from [12], and the lines are the distributions that we obtain at several different times during the collision

3.2.2 Momentum Dependent EoS

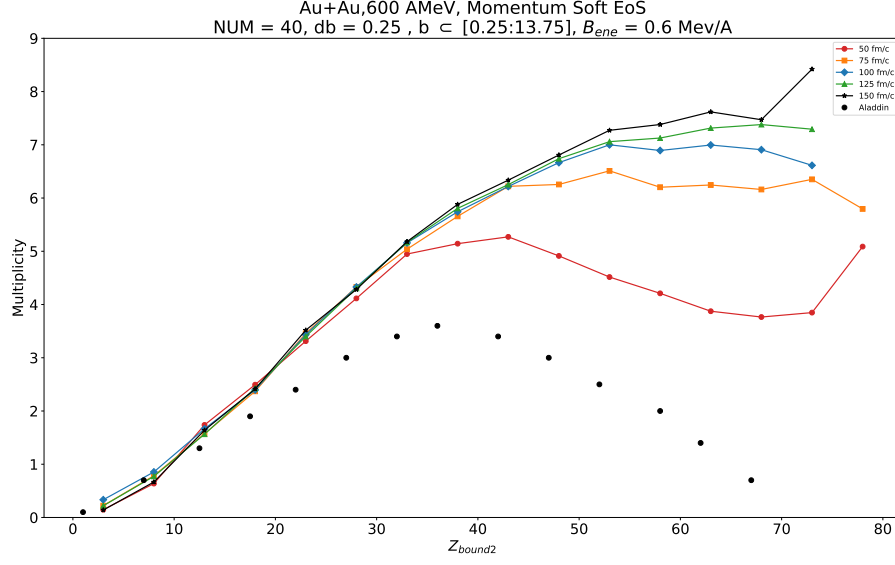Finally we can see how well our Momentum dependent interaction functions.

Figure 3.3: Fragment distribution in number as a function of the charge contained, the dots are the experimental values that were obtained from [12], and the lines are the distributions that we obtain at several different times during the collision

As we can see the momentum dependent has a similar behaviour to that of the static soft version, meaning that the potential is more prone to cluster the nuclei together after the collision
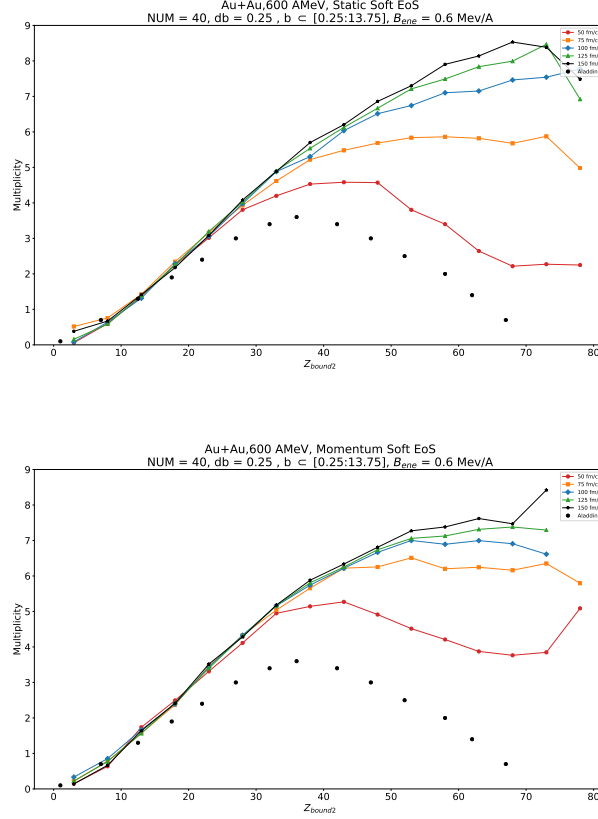
Figure 3.4: Fragement distribution for the Soft static(top), compared to the momentum dependent (bottom)

Comparing with the soft EoS we can see that the cluster formation is even more pronouced and larger in number. Historically the MDI has always been troublesome to implement because of unforseen interactions that make it stronger than expected.

3.3 Flow

The section experimentally verifiable quantity is the flow. Anisotropic proton and neutron flow in the nuclei occurs during the collision. The two kinds that we shall briefly mention are v_1 direct flow and v_2 elliptical flow defined as :

$$v_1 = \left\langle \frac{p_x}{\sqrt{p_x^2 + p_y)^2}} \right\rangle = \left\langle \cos(\phi) \right\rangle \tag{3.1}$$

$$v_2 = \left\langle \frac{p_x^2 - p_y^2}{p_x^2 + p_y^2} \right\rangle = \left\langle \cos(2\phi) \right\rangle \tag{3.2}$$

CHAPTER 4

CONCLUSION

BIBLIOGRAPHY

[1] *Vlasov-Uehling-Uhlenbeck theory of medium energy heavy ion reactions: Role of mean field dynamics and two body collisions*. Kruse, B. V. Jacak, J. J. Molitoris, G. D. Westfall, and H. Stöcker

[2] *Numerical simulation of medium energy heavy ion reactions* J. Aichelin and G. Bertsch

[3] *Production of deuterons and pions in a transport model of energetic heavy-ion reactions* P.Danielewicz G.F.Bertsch

[4] *Multiphase transport model for relativistic heavy ion collisions* Zi-Wei Lin, Che Ming Ko, Bao-An Li, Bin Zhang, and Subrata Pal

[5] *Hadronic and electromagnetic probes of hot and dense nuclear matter* W.Cassing E.L.Bratkovskaya

[6] *Transport-theoretical description of nuclear reactions* O.Buss T.Gaitanos K.Gallmeister H.van Hees M.Kaskulov O.Lalakulich A.B.Larionov T.Leitner J.Weil U.Mosel

[7] *Particle production and equilibrium properties within a new hadron transport approach for heavy-ion collisions* J. Weil, V. Steinberg, J. Staudenmaier, L. G. Pang, D. Oliinychenko, J. Mohs, M. Kretz, T. Kehrenberg, A. Goldschmidt, B. Bäuchle, J. Auvinen, M. Attems, and H. Petersen

[8] *Modelling the many-body dynamics of heavy ion collisions: Present status and future perspective* C. Hartnack Rajeev K. Puri J. Aichelin J. Konopka S.A. Bas sH. Stöcker W. Greiner

[9] *Microscopic Models for Ultrarelativistic Heavy Ion Collisions* S. A. Bass, M. Belkacem, M. Bleicher, M. Brandstetter, L. Bravina, C. Ernst, L. Gerland, M.

Hofmann, S. Hofmann, J. Konopka, G. Mao, L. Neise, S. Soff, C. Spieles, H. Weber, L. A. Winckelmann, H. Stöcker, W. Greiner, Ch. Hartnack, J. Aichelin, N. Amelin

[10] *Relativistic Hadron-Hadron Collisions in the Ultra-Relativistic Quantum Molecular Dynamics Model (UrQMD)* M. Bleicher, E. Zabrodin, C. Spieles, S.A. Bass, C. Ernst, S. Soff, L. Bravina, M. Belkacem, H. Weber, H. Stöcker, W. Greiner

[11] *New parametrization of the optical potential* C. Hartnack and J. Aichelin

[12] *Universality of spectator fragmentation at relativistic bombarding energies* A. Schuttauf et al., Nucl. Phys. A 607

[13] *Systematics of central heavy ion collisions in the 1A GeV regime* FOPI Collaboration: W. Reisdorf et al

[14] *Parton transport and hadronization from the dynamical quasiparticle point of view* W. Cassing, E.L. Bratkovskaya

[15] *Parton-Hadron-String Dynamics: an off-shell transport approach for relativistic energies* W. Cassing, E.L. Bratkovskaya

[16] *'Quantum' molecular dynamics: A Dynamical microscopic n body approach to investigate fragment formation and the nuclear equation of state in heavy ion collisions* J. Aichelin

[17] *Preliminary Results from the Parton-Hadron-Quantum-Molecular Dynamics (PHQMD) Transport Approach* J. Aichelin , E. Bratkovskaya, A. Le Fèvre, V. Kireyev , Y. Leifels